Scientific Research

PID-Type Fuzzy Controller for Grid-Supporting Inverter of Battery in Embedded Small Variable Speed Wind Turbine

Ferdian Ronilaya[1,2], Hajime Miyauchi[1], Adi Kurniawan[3]

[1]Department of Frontier Technology for Energy and Devices, Kumamoto University, Kumamoto-shi, Japan
[2]Department of Electrical Power Engineering, The State Polytechnic of Malang, Malang, Indonesia
[3]Institut Teknologi Sepuluh Nopember, Surabaya, Indonesia
Email: ferdian@st.cs.kumamoto-u.ac.jp

Abstract

Frequency and voltage of embedded variable speed wind turbine (VSWT) driving a permanent magnet synchronous generator (PMSG) is strongly affected by wind speed fluctuations. In practice, power imbalance between supply and demand is also common, especially when VSWT-PMSG is connected to a weak micro grid (MG). If load demand fluctuations become high, isolated MG may be unable to stabilize the frequency and voltage so that battery storage needs to be installed into the MG to adjust energy supply and demand. To allow flexible control of active and reactive power flow from/to battery storage, grid-supporting inverters are used. For a system that contains highly nonlinear components, the use of conventional linear proportional-integral-derivative (PID) controllers may cause system performance deterioration. Additionally, these controllers show slow, oscillating responses, and complex equations are required to obtain optimum responses in other controllers. To cope with these limitations, this paper proposes PID-type fuzzy controller (PIDfc) design to control grid-supporting inverter of battery. To ensure safe battery operating limits, we also propose a new controller scheme called intelligent battery protection (IBP). This IBP is integrated into PIDfc. Several simulation tests are performed to verify the scheme's effectiveness. The results show that the proposed PIDfc controller exhibits improved performance and acceptable responses, and can be used instead of conventional controllers.

1. Introduction

VSWT-PMSG is a promising wind turbine system due to its ability to extract maximum power from fluctuating

wind resources. PMSG can operate at low wind speeds so that a gearbox is no longer needed. This feature may reduce the cost and is suitable for small-scale applications. The VSWT-PMSG power varies with the wind speed, so this can lead to poor performance of frequency and voltage of MG [1]. To obtain better performance, both in terms of technical and economical, VSWT-PMSG needs some reliable control strategies. This is usually done with the help of power electronics devices, for example an inverter. In most cases in the distributed generations (DG), the inverter is connected in parallel with other inverters so that the inverter controller should be designed appropriately.

Many researchers have considered the control strategies of parallel-connected inverters [2-5]. Most control strategies are based on the droop method. Use of this method for inverter control was proposed by Chandorkar *et al.* [3]. Their goal was to have accurate load sharing among the inverters. Parallel inverter operation was also discussed by Kawabata *et al.* [4]. However, this study only focused on safe inverter operation. The dynamic voltage and frequency responses of the output inverters were not discussed. Control strategies for nonlinear load sharing by regulating the inverter output voltage bandwidth have been proposed [6]. Novel control structures that include virtual resistors and reactors to adjust the output impedance were developed in [7,8], respectively. However, these control strategies have two limitations. First, there is a trade-off between voltage regulation and load sharing. Second, the proposed controllers have slower dynamic responses. To overcome these limitations, a new control strategy was proposed by Guerrero *et al.* [9]. The scheme uses a wireless controller by including a supplemental transient droop characteristic in the conventional static droop method. However, the main problem of this scheme lies in the measurement noise and proportional load sharing accuracy. The first problem was overcome using *H-∞* controllers [10-12]. But, the main drawback of this controller for real implementation is that the *H-∞* technique requires high levels of mathematical understanding [13]. The second limitation of the droop controller proposed in [9] was overcome by Qing-Chang [14]. However, for a system that contains highly nonlinear components, the use of linear conventional PID controllers may weaken the system performance.

Rather than using high levels of mathematical understanding, this paper proposes a simple method based on PIDfc to define the relationship between input information and output action. Furthermore, fuzzy-based controller is suitable for highly non-linear components. Based on the literature review carried out by Pandey *et al.* [15], however, little research has been conducted in this area. Similar studies were discussed in [16]. However, grid-connected inverter control, which is the subject of this work, has not been discussed. Additionally, voltage control is not taken into account.

As flooded deep-cycle lead-acid batteries are used, safe battery operation should be considered in designing controller of the grid-supporting inverter. The battery should not be overcharged or overdischarged because it may shorten the battery life and damage the battery. To accommodate these limitations, we propose a new controller strategy scheme called intelligent battery protection (IBP). The SOC (state of charge) is used as input signal in the IBP scheme. The output of IBP acts as intelligent protection signal which is then sent to PIDfc as additional input.

2. System Model

Figure 1 shows the configuration of isolated embedded VSWT system. It is assumed that this prototype is used for non-urban electrification and is located on coastal area with flat terrain. MG/diesel generator behaves as the main power supply and has 31 kVA capacity. All of the energy sources are used to meet dynamic household and agricultural electricity demand.

2.1. VSWT-PMSG Characteristics and Modeling

The wind turbine model used in this simulation is manufactured by Fortis Wind Energy. It has 7-meter span blades. The company claims that this turbine can generate 10 kW of power at 13 m/s of wind speed [17]. The *v-P* (wind speed-power) characteristic of this turbine is shown in **Figure 2**. By using polynomial regression, such a characteristic can be modeled by (1).

$$P_w = -1.1v^4 + 24.3v^3 - 61.8v^2 + 41.5v - 9.5 \tag{1}$$

where *v* is wind speed in m/s and P_w is wind turbine power. The tower on which the wind turbine is mounted has 30 m height and is located on 5 m from MG bus.
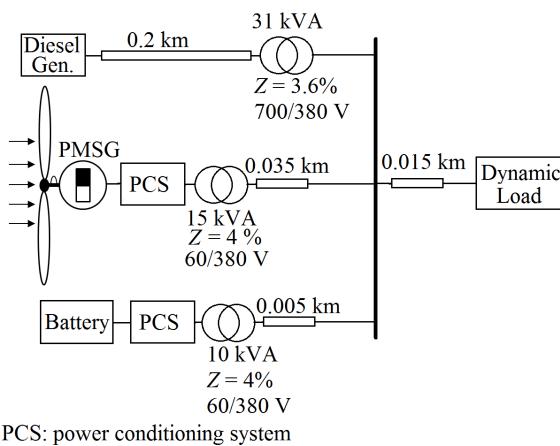
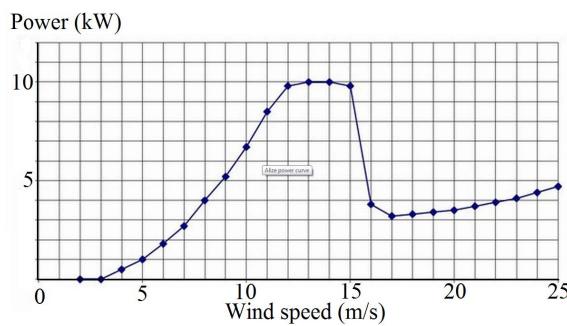**Figure 1.** Isolated MG with embedded small VSWT-PMSG and batteries.

Figure 2. Alize Fortis wind turbine characteristics.

2.2. Lead-Acid Battery Model

The non-linear dynamic model of lead acid battery used is adopted from [18,19] and is available in Matlab/Simpowersystem library. **Table 1** lists the parameters used in the simulation.

One of important parameters of lead acid battery is SOC. SOC represents available energy capacity of the lead acid battery. In this paper, the SOC value is limited between 30% - 90% and is used as one of primary input signals of IBP.

3. Inverter Control

The output impedance of the inverter is usually very inductive, $Z\angle\theta = X\angle90°$, therefore, the flow of real and reactive power from grid-connected inverters can be expressed by (3) and (4) [9].

$$P = \frac{EV}{X}\sin\delta \tag{2}$$

$$Q = \frac{EV\cos\delta - V^2}{X} \tag{3}$$

P: active power
Q: reactive power
X: output reactance of inverter
E: output voltage of inverter
V: MG bus voltage
δ: phase angle between *E* and *V*
Based on (2) and (3), the active and reactive power is predominantly be affected by the value of phase angle,

δ and inverter output voltage, E, respectively. In other words, by adjusting P and Q, the frequency and voltage can be determined.

3.1. VSWT-PMSG Inverter Controller

Figure 3 shows a schematic diagram of the proposed inverter controller of the VSWT-PMSG. The use of PMSG can provide some major simplifications because it does not require excitation current so as to save costs and improve efficiency [20]. Voltage and frequency output of VSWT-PMSG fluctuate with wind speed so that the output of VSWT-PMSG need to be converted into DC voltage by using rectifier and is stabilized by synchronous buck converter. The PMSG and rectifier are completely uncontrollable. Thus, active and reactive power transfer can only be realized by controlling the inverter.

For a given MG bus voltage, based on (2) and (3), the real and reactive power can be controlled by regulating the angle δ and amplitude of inverter output voltage, E. The regulation can be realized by varying the sinusoidal reference magnitude, U and phase angle, δ_w, with respect to the MG voltage. The frequency of sinusoidal modulating reference signal must equal to that of MG. Therefore, signal from PLL (ωt) is used as reference. Limiter L_v is used to limit the amplitude of reference voltage U not higher than that of the carrier voltage. VSWT-PMSG is operated under unity power factor so that reactive power reference is set to 0.

The rated wind speed for the VSWT-PMSG is 13 m/s. If the wind speed is higher than 13 m/s, VSWT-PMSG power is limited at the rated power value. A limiter Lf is used to realize this strategy. Below the rated wind speed, the VSWT-PMSG follows the power output conditions as it is defined in (1).

3.2. Battery Inverter Controller

PIDfc is first introduced by Wu Zhi and Mizumoto in 1996 [21]. The interesting feature of this controller scheme is that it is quite simple and has reduced overshoot if the gain factors are selected properly. The implementation of PIDfc scheme in the inverter controller is shown in **Figure 4**. Two PIDfc blocks are used to regulate frequency and voltage of the MG. The PIDfc scheme is designed such that the deviation of the frequency

Table 1. The battery parameters.

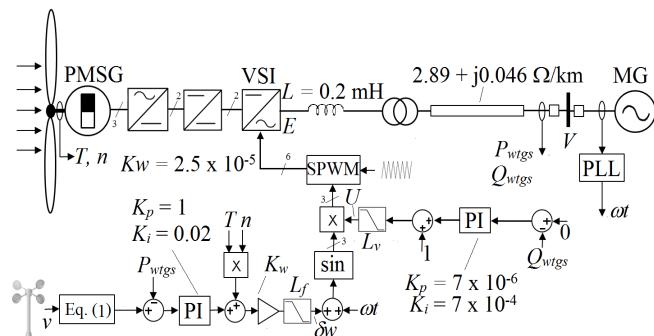| Parameters	Value
Internal resistance	0.008 ohm
Fully charge voltage	261.3158 V
Exponential voltage zone	244.34 V
Exponential capacity zone	1 Ah
Maximum capacity	312.5 Ah
Nominal discharge current	60 A
Capacity at nominal voltage	93.0833 Ah

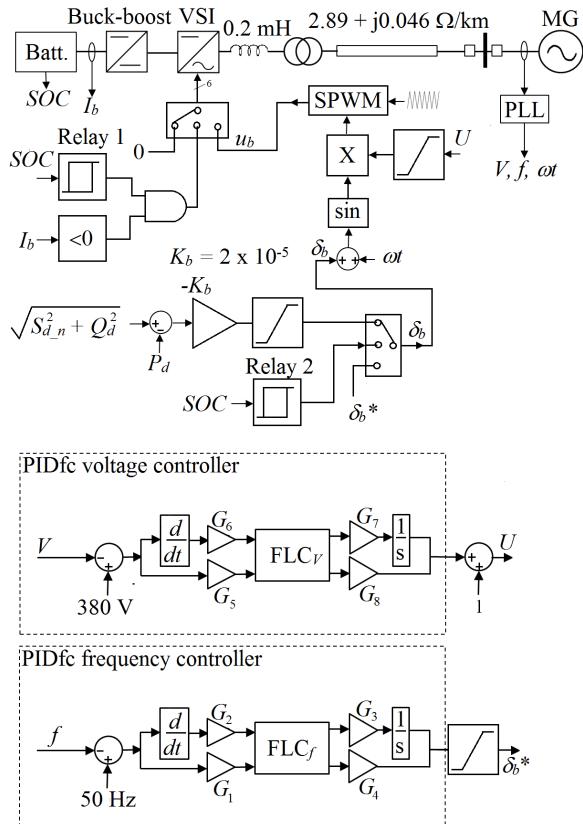**Figure 3.** VSWT-PMSG inverter controller.

Figure 4. Battery inverter controller.

and voltage of the MG does not exceed 2% and 5% respectively [9]. **Figure 5** shows input and output membership functions (MFs) of FLC*f* and FLC*v*. The rule bases table for both FLC*f* and FLC*v* is listed in **Table 2**. IBP is realized by using two hysteresis relays (Relay 1 and 2). Relay 1 is used to protect the battery from overcharge condition. Relay 1 will be ON only if the SOC of the battery is equal to 90%. It remains ON until the SOC drops to 80%. When the SOC is equal to 90% and the battery current is negative, then the battery is disconnected from the MG. Meanwhile, Relay 2 is intended to protect the battery from over-discharge conditions. If the SOC is equal to 30%, Relay 2 will be ON. With this condition, the controller will force the battery to absorb electrical power from MG whose value is proportional to the available power from diesel generators. Available power from diesel generator can be expressed by (4).
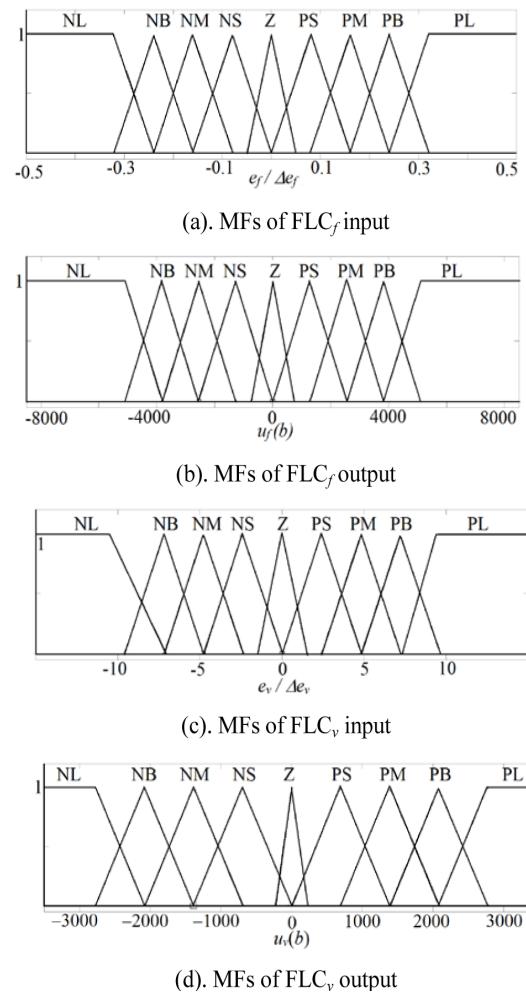
$$P_{av.} = \sqrt{S_{d\_n}^2 - Q_d^2} - P_d \tag{4}$$

S_{d_n} is nominal power capacity of diesel generator (31 kVA). Meanwhile, Q_d and P_d are measured reactive and active power of diesel generator respectively. To prevent excessive charging current, limiter block is used. It should be noted that Relay 2 will remain ON until the SOC of the battery rises to 50%.

4. Simulation Results

Several simulation tests are performed to verify the performance of proposed PIDfc controller. Then, the simulation results of PIDfc are compared with that of conventional PID controller. To analyze the significance of battery in regulating frequency and voltage of MG, the simulation results are also compared with that of the system in which the battery is not used. Load changes dynamically with constant power factor, *i.e.* 0.93. To obtain best performance, parameters of PIDfc and conventional PID controllers for all simulation cases are obtained by using trial-and-error method. The parameters of PIDfc controller are listed in **Table 3**. Matlab/Simpower system software is used to simulate the model.
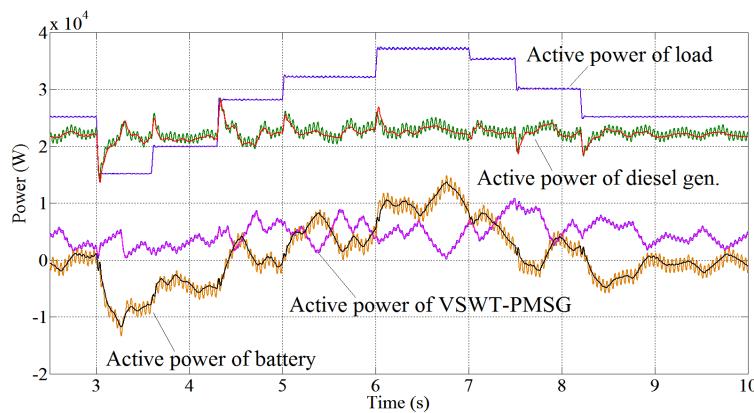
Active power profiles of diesel generator, VSWT-PMSG, battery and load are shown in **Figure 5**. Meanwhile

(a). MFs of FLC$_f$ input

(b). MFs of FLC$_f$ output

(c). MFs of FLC$_v$ input

(d). MFs of FLC$_v$ output

Figure 5. MFs of FLC$_f$ and FLC$_v$.

Table 2. The Rules Base for FLC$_f$ and FLC$_v$.

Δef \ ef	NL	NB	NM	NS	Z	PS	PM	PB	PL
NL	NL	NL	NL	NL	NL	NB	NM	NS	Z
NB	NL	NL	NL	NL	NB	NM	NS	Z	PS
NM	NL	NL	NL	NB	NM	NS	Z	PS	PM
NS	NL	NL	NB	NM	NS	Z	PS	PM	PB
Z	NL	NB	NM	NS	Z	PS	PM	PB	PL
PS	NB	NM	NS	Z	PS	PM	PB	PL	PL
PM	NM	NS	Z	PS	PM	PB	PL	PL	PL
PB	NS	Z	PS	PM	PB	PL	PL	PL	PL
PL	Z	PS	PM	PB	PL	PL	PL	PL	PL

Table 3. The PIDfc parameters.

Parameters	Value
G_1	1
G_2	2
G_3	5×10^{-4}
G_4	3×10^{-6}
G_5	1
G_6	1
G_7	5×10^{-4}
G_8	2×10^{-5}
K_b	2×10^{-5}

Figure 5. Active power profiles.

the reactive power and battery current responses are shown in **Figures 6** and **7** respectively. The oscillating responses are the simulation results when the conventional PID controller is used. On the other hand, smoother responses are the results of PIDfc. These results confirm that PIDfc exhibits improved performance than that of conventional PID controller. The sudden load changes are compensated by diesel generator because it can absorb or deliver power faster than the battery. The negative value of battery current indicates that the battery is being charged and vice versa. We can see from **Figure 7** that the maximum current of the battery is equal to 60 A which confirms to the nominal discharge current value listed in **Table 1**.

The active power delivered by VSWT-PMSG is proportional to the *v-P* characteristics as defined in **Figure 2** and (1). In other hand, the reactive power delivered from VSWT-PMSG is equal to 0. It indicates the VSWT-PMSG is operating at unity power factor as aforementioned design in Section 3.1.

Figures 8 and **9** show the frequency and voltage profiles for both using PIDfc and conventional PID controller. To verify the effectiveness of PIDfc controller quantitatively, the following performance index is used:

$$ISE = \int_0^T |e|^2 dt \tag{5}$$

ISE is integral squared error. Meanwhile, *e* and *T* are frequency/voltage error and simulation time respectively. **Table 4** summarizes the calculated *ISE* of MG frequency and voltage for different conditions.

This table verifies that PIDfc shows better performance than conventional PID controller, as shown in the lower value of ISE for both voltage and frequency. Moreover, this table signifies that the battery plays an important role particularly when power unbalance between supply and demand occurs in isolated MG system. Battery may also provide a way to operate diesel generator in more efficient manner. Any extra power can be used
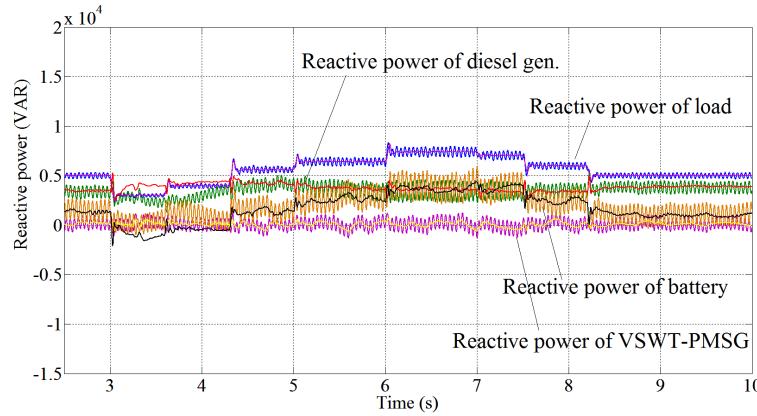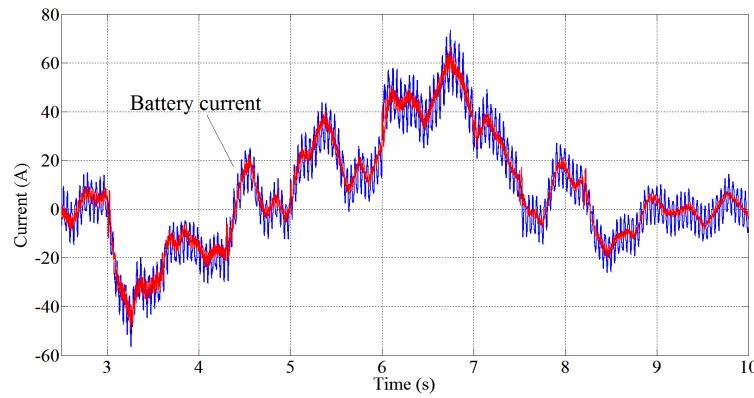
Figure 6. Reactive power profiles.

Figure 7. Battery current profiles.

Table 4. The calculated *ISE*.

Parameters	ISE
Frequency (PIDfc based)	0.021617
Frequency (PID based)	0.037741
Frequency (wthout battery support)	21.10304
Voltage (PIDfc based)	5.454813
Voltage (PID based)	14.34414
Voltage (without battery support)	1018.58

to charge the battery during low load time and energy can be extracted during peak times. Although the initial cost of the battery installation is expensive, fuel savings are much greater than the initial extra cost for remote area application.

5. Conclusion

In this paper, a PIDfc controller for battery grid-supporting inverter in embedded VSWT-PMSG has been presented. In order to protect the battery from overcharge and overdischarge condition, IBP is introduced and integrated with PIDfc controller. Simulation results show that PIDfc has lower *ISE* than that of conventional PID controller. It indicates that PIDfc exhibits significantly improved performance and can be used instead of conventional controllers.
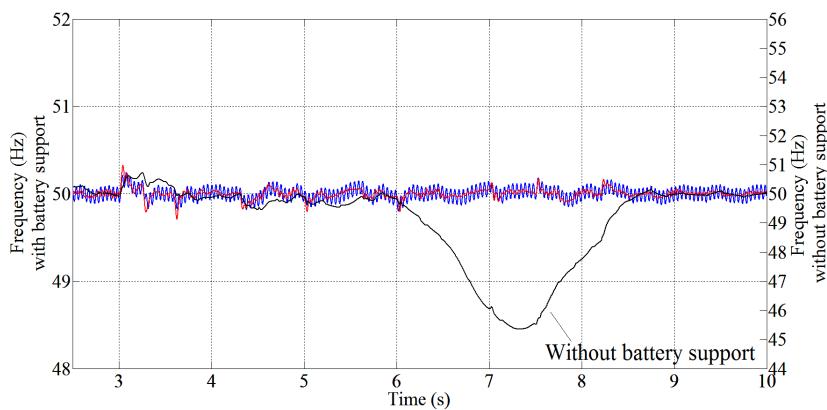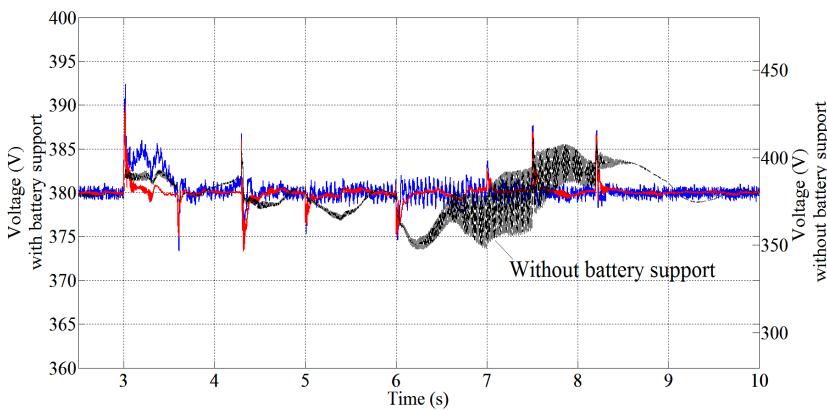
Figure 8. Frequency profiles.

Figure 9. Voltage profiles.

Acknowledgements

References

[1] Muyeen, S.M., Takahashi, R., Murata, T. and Tamura, J. (2009) Integration of an Energy Capacitor System with a Variable-Speed Wind Generator. *IEEE Transactions on Energy Conversion*, **24**, 740-749.
http://dx.doi.org/10.1109/TEC.2009.2025323

[2] Barsali, S., Ceraolo, M., Pelacchi, P. and Poli, D. (2002) Control Techniques of Dispersed Generators to Improve the Continuity of Electricity Supply. *IEEE Power Engineering Society Winter Meeting*, 789-794.
http://dx.doi.org/10.1109/PESW.2002.985115

[3] Chandorkar, M.C., Divan, D.M. and Adapa, R. (1993) Control of Parallel Connected Inverters in Standalone AC Supply Systems. *IEEE Transactions on Industry Applications*, **29**, 136-143. http://dx.doi.org/10.1109/28.195899

[4] Kawabata, T. and Higashino, S. (1988) Parallel Operation of Voltage Source Inverters. *IEEE Transactions on Industry Applications*, **24**, 281-287. http://dx.doi.org/10.1109/28.2868

[5] Matthias, H. and Helmut, S. (2002) Control of a Three Phase Inverter Feeding an Unbalanced Load and Operating in Paralel with Other Power Sources. EPE-PEMC, Dubrovnik & Cavtat, 1-10.

[6] Tuladhar, A., Jin, K., Unger, T. and Mauch, K. (1997) Parallel Operation of Single Phase Inverter Modules with No Control Interconnections. *Twelfth Annual APEC*, 23-27 Feb 1997, 94-100.
http://dx.doi.org/10.1109/APEC.1997.581439

[7] Chiang, S.J., Yen, C.Y. and Chang, K.T. (2001) A Multimodule Parallelable Series-Connected PWM Voltage Regulator. *IEEE Transactions on Industrial Electronics*, **48**, 506-516. http://dx.doi.org/10.1109/41.925577

[8]   Engler, A. (2000) Control of Parallel Operating Battery Inverters. PV Hybrid Power System.

[9]   Guerrero, J.M., Garcia de Vicuna, L., Matas, J., Castilla, M. and Miret, J. (2004) A Wireless Controller to Enhance Dynamic Performance of Parallel Inverters in Distributed Generation Systems. *IEEE Transactions on Power Electronics*, **19**, 1205-1213. http://dx.doi.org/10.1109/TPEL.2004.833451

[10]   Goya, T., Omine, E., Kinjyo, Y., Senjyu, T., Yona, A., Urasaki, N. and Funabashi, T. (2011) Frequency Control in Isolated Island by Using Parallel Operated Battery Systems Applying H-Inf; Control Theory Based on Droop Characteristics. *IET Renewable Power Generation*, **5**, 160-166. http://dx.doi.org/10.1049/iet-rpg.2010.0083

[11]   Patra, S., Sen, S. and Ray, G. (2007) Design of Robust Load Frequency Controller: H_∞ Loop Shaping Approach. *Electric Power Components and Systems*, **35**, 769-783. http://dx.doi.org/10.1080/15325000601175140

[12]   Singh, V.P., Mohanty, S.R., Kishor, N. and Ray, P.K. (2013) Robust H-Infinity Load Frequency Control in Hybrid Distributed Generation System. *International Journal of Electrical Power & Energy Systems*, **46**, 294-305,. http://dx.doi.org/10.1016/j.ijepes.2012.10.015

[13]   Cubillos, X.C.M. and Souza, L.C.G.D. (2009) Using H-Infinity Control Method in Attitude Control System of Rigid-Flexible Satellite. *Mathematical Problems in Engineering*, **2009**, 1-9. http://dx.doi.org/10.1155/2009/173145

[14]   Qing-Chang, Z. (2013) Robust Droop Controller for Accurate Proportional Load Sharing among Inverters Operated in Parallel. *IEEE Transactions on Industrial Electronics*, **60**, 1281-1290. http://dx.doi.org/10.1109/TIE.2011.2146221

[15]   Pandey, S.K., Mohanty, S.R. and Kishor, N. (2013) A Literature Survey on Load-Frequency Control for Conventional and Distribution Generation Power Systems. *Renewable and Sustainable Energy Reviews*, **25**, 318-334. http://dx.doi.org/10.1016/j.rser.2013.04.029

[16]   Yeşil, E., Güzelkaya, M. and Eksin, I. (2004) Self Tuning Fuzzy PID Type Load and Frequency Controller. *Energy Conversion and Management*, **45**, 377-390. http://dx.doi.org/10.1016/S0196-8904(03)00149-3

[17]   Fortis Wind Energy (2013) Alize Wind Turbine. http://www.fortiswindenergy.com/products/wind-turbines/alize

[18]   Matlab/Simpowersystem (2013) Battery-Implement Generic Battery Model. http://www.mathworks.com/help/physmod/powersys/ref/battery.html

[19]   Tremblay, O. and Dessaint, L.A. (2009) Experimental Validation of a Battery Dynamic Model for EV Application. *World Electric Vehicle Journal*, **3**, 1-10.

[20]   Chen, Z. and Spooner, E. (1998) Grid Interface Options for Variable-Speed, Permanent-Magnet Generators. *IEE Proceedings*: *Electric Power Applications*, **145**, 273-283. http://dx.doi.org/10.1049/ip-epa:19981981

[21]   Wu, Z.Q. and Mizumoto, M. (1996) PID Type Fuzzy Controller and Parameters Adaptive Method. *Fuzzy Sets and Systems*, **78**, 23-35. http://dx.doi.org/10.1016/0165-0114(95)00115-8